TISSUE ENGINEERING: Part A
Volume 20, Numbers 3 and 4, 2014

DOI: 10.1089/ten.tea.2013.0229

Bone Regeneration Potential of Stem Cells Derived from Periodontal Ligament or Gingival Tissue Sources Encapsulated in RGD-Modified Alginate Scaffold

Alireza Moshaverinia, DDS, MS, PhD,[1] Chider Chen, BSc, MSc,[1] Xingtian Xu, DDS,[1]
Kentaro Akiyama, DDS, PhD,[1] Sahar Ansari, MSc,[2]
Homayoun H. Zadeh, DDS, PhD,[2] and Songtao Shi, DDS, PhD[1]

Mesenchymal stem cells (MSCs) provide an advantageous alternative therapeutic option for bone regeneration in comparison to current treatment modalities. However, delivering MSCs to the defect site while maintaining a high MSC survival rate is still a critical challenge in MSC-mediated bone regeneration. Here, we tested the bone regeneration capacity of periodontal ligament stem cells (PDLSCs) and gingival mesenchymal stem cells (GMSCs) encapsulated in a novel RGD- (arginine-glycine-aspartic acid tripeptide) coupled alginate microencapsulation system *in vitro* and *in vivo*. Five-millimeter-diameter critical-size calvarial defects were created in immunocompromised mice and PDLSCs and GMSCs encapsulated in RGD-modified alginate microspheres were transplanted into the defect sites. New bone formation was assessed using microcomputed tomography and histological analyses 8 weeks after transplantation. Results confirmed that our microencapsulation system significantly enhanced MSC viability and osteogenic differentiation *in vitro* compared with non-RGD-containing alginate hydrogel microspheres with larger diameters. Results confirmed that PDLSCs were able to repair the calvarial defects by promoting the formation of mineralized tissue, while GMSCs showed significantly lower osteogenic differentiation capability. Further, results revealed that RGD-coupled alginate scaffold facilitated the differentiation of oral MSCs toward an osteoblast lineage *in vitro* and *in vivo*, as assessed by expression of osteogenic markers Runx2, ALP, and osteocalcin. In conclusion, these results for the first time demonstrated that MSCs derived from orofacial tissue encapsulated in RGD-modified alginate scaffold show promise for craniofacial bone regeneration. This treatment modality has many potential dental and orthopedic applications.

Introduction

The ultimate goal of bone tissue engineering is to regenerate a construct that matches the physical and biological properties of natural bone tissue.[1] Autologous and allogenic bone grafts currently comprise about 90% of grafts performed each year. However, these treatment modalities are expensive due to the high cost of bone-harvesting procedures and are associated with donor site morbidity, hematomas, inflammation, and pain.[1,2] Tissue regeneration using mesenchymal stem cells (MSCs) presents several advantages over grafts, including high-quality regeneration of damaged tissues without the formation of fibrous tissue, no donor-site harvesting, and low risk of disease transmission or autoimmune rejection due to the immunoregulatory capacity of MSCs.[3] It is well known that MSCs reside in a wide spectrum of postnatal tissue types, including the dental and orofacial tissues.[4,5] MSCs derived from orofacial tissues are proliferative postnatal stem cells capable of differentiating into odontogenic, adipogenic, and osteogenic tissues.[4–6] Additionally, the neural crest origin of these MSCs makes them attractive for craniofacial regenerative strategies as they might be more plastic to differentiate into craniofacial tissues.[4–7] Moreover, studies have shown that dental-derived MSCs may have superior differentiation capacities when compared with human bone marrow mesenchymal stem cells (hBMMSCs).[4–7] Therefore, orofacial-derived MSCs, in combination with suitable scaffolds, are able to differentiate into desirable tissue phenotypes, and are promising candidates for numerous regenerative therapeutic applications.[8,9] Among the different types of dental MSCs that have been identified so far, stem cells from periodontal

[1]Center for Craniofacial and Molecular Biology (CCMB), Ostrow School of Dentistry, University of Southern California, Los Angeles, California.
[2]Laboratory for Immunoregulation and Tissue Engineering (LITE), Ostrow School of Dentistry, University of Southern California, Los Angeles, California.

ligaments (PDLSCs) and gingival mesenchymal stem cells (GMSCs) are of special interest. For instance, GMSCs, and to some extent PDLSCs, are readily accessible in the oral environment and can also be readily found in discarded tissue samples. Studies have confirmed the multilineage differentiation capacity of these stem cells *in vitro* and *in vivo*.[10–12] Specifically, it has been reported that PDLSCs are capable of regenerating a typical cementum and/or periodontal-ligament-like structure *in vivo*.[10,11] Other studies have suggested that GMSCs could be used for therapeutic clinical applications such as MSC-based bone reconstruction.[12,13]

Although there are many scaffold-free stem cell delivery strategies (e.g., cell sheet engineering) with promising clinical outcomes,[14] it is well known that the cell delivery vehicle plays an important role in the *in vivo* performance of MSCs and dictates the success of the regenerative therapy.[15,16] Studies have confirmed that providing a suitable microenvironment for MSC proliferation and differentiation in response to exogenous stimuli and growth factors is a critical step toward clinical applications.[17–23] Several types of scaffolds have been used to support growth and differentiation of progenitor cells for bone regeneration, including natural polymers (e.g., alginates).[23,24] Alginates are natural heteropolysaccharides that are isolated from brown sea algae.[25,26] Due to their unique properties including gentle gelation behavior, biodegradability, biocompatibility, easy cell encapsulation/cell recovery, and chemical versatility, they have a wide variety of biomedical applications, such as the encapsulation of cells and sensitive bioactive molecules to facilitate minimally invasive surgical procedures.[27–29] In our previous studies, we have utilized alginate hydrogels as a scaffold for the encapsulation of PDLSCs and GMSCs.[19,20] We showed that an alginate encapsulation system has the potential to enhance hard tissue regeneration *in vitro* and *in vivo*, making it a promising candidate for minimally invasive dental and orthopedic applications.[19,20] However, one of the disadvantages of the earlier-mentioned MSC-alginate encapsulation system is the impaired proliferation and differentiation of encapsulated MSCs due to hypoxia. One likely reason for this is the large diameter of the capsules ($>500\,\mu m$), which makes the diffusion of nutrients and oxygen to the cells in the center of the spheres deficient and leads to decreased cell viability.[30–32] Thus, a technique that can create smaller microbeads to enhance diffusion and therefore cell viability is desirable. Microfluidic technology holds promise for such an approach, enabling the formation of microspheres with $<500\,\mu m$ diameter and a very narrow particle size distribution.[33,34]

In addition to decreasing the size of the microbeads, it is also desirable to find biomaterials with improved bioactivity to make an optimal scaffold for the encapsulation of MSCs. It is well known that bone extracellular matrix (ECM) components play a crucial role in controlling osteoblast gene expression through interaction with cell-surface receptors of the integrin family.[35–37] Therefore, it is advantageous to utilize cell-binding peptides, such as RGD (arginine-glycine-aspartic acid tripeptide), in the structure of the alginate scaffold to mimic the cell-interactive function of the ECM. The RGD tripeptide sequence is an adhesion motif found in ECM proteins (e.g., fibronectin). It has been reported that several integrin receptors, such as avb3 and a5b1, have the capacity to bind directly to RGD.[36–38] RGD-coupled alginate scaffolds therefore provide a favorable physiochemical microenvironment by presenting ligands that specifically bind to cell receptors.[38–41] However, a literature search revealed no reports that assess the bone regenerative capacity of encapsulated PDLSCs and GMSCs in RGD-coupled alginate microspheres. Indeed, overall in comparison to other dental-derived MSCs, these two easily accessible stem cell sources have not been studied widely. Therefore, the objective of this study was to develop a construct composed of biodegradable and injectable RGD-coupled alginate microspheres encapsulating PDLSCs and GMSCs using microfluidic technology, and to assess the bone regeneration potential of dental MSCs encapsulated in this fashion. It was hypothesized that the bone regeneration capacity of PDLSCs and GMSCs encapsulated in RGD-coupled alginate microspheres of a small diameter would be greatly enhanced, making this a promising combination for various bone tissue engineering applications.

Materials and Methods

Progenitor cell isolation and culture

Human PDLSCs, GMSCs, and hBMMSCs were isolated and cultured according to previously published protocols by Seo *et al.*[5] and Zhang *et al.*[7] The teeth and gingival tissues were obtained from healthy male patients (18–25 years old) without any history of periodontal disease who were undergoing third molar extractions, under IRB approval from the University of Southern California (BUA6510). Briefly, periodontal ligament tissues were gently separated from the surface of the root and digested in a collagenase type I solution (Worthington Biochem) and dispase (Roche) for 1 h at 37°C. Single-cell suspensions were obtained by passing the cells through a 70-μm strainer (Falcon; BD Labware). To identify the PDLSCs, these single-cell suspensions (1×10^4 cells) were seeded into 10-cm culture dishes (Costar) with α-minimum essential medium (MEM) (GIBCO BRL) supplemented with 15% fetal calf serum (Equitech-Bio, Inc.), 100 μM ascorbic acid 2-phosphate (Sigma-Aldrich), 2 mM glutamine, 100 U/mL penicillin, and 100 μg/mL streptomycin (Sigma-Aldrich), and then incubated at 37°C in 5% CO_2.[5]

For extraction of GMSCs, gingival tissues were treated aseptically and incubated overnight at 4°C with dispase (2 mg/mL; Sigma-Aldrich). Next, the tissues were minced into small fragments and digested in collagenase IV solution (Worthington Biochem) in sterile phosphate-buffered saline (PBS) at 37°C for 2 h. The retrieved cell suspension was then filtered through a 70-μm cell strainer (Falcon). Afterward, the cells were cultured in 10-cm culture dishes with α-MEM supplemented with 15% fetal calf serum, 100 μM ascorbic acid 2-phosphate, 2 mM glutamine, 100 U/mL penicillin, 100 μg/mL streptomycin, and 550 μM 2-mercaptoethanol; and then incubated at 37°C in 5% CO_2.[7] After 72 h, the nonadherent cells were removed and the plastic-adherent confluent cells were passaged for future use. For the colony-forming unit–fibroblastic (CFU-F) assay, 0.1×10^6 cells were seeded in a culture dish and cultured for 14 days, and then stained with toluidine blue. A count of more than 50 cells in one colony was counted as positive on the CFU-F assay.[4] Passage 4 cells were used in the experiments and hBMMSCs were used as the positive control group.

Flow cytometric analysis

Approximately 5×10^5 cells from passages 2–6 were incubated with specific phycoerythrin- or fluorescein isothiocyanate-conjugated mouse monoclonal antibodies for human CD34 (as negative hematopoietic stem cell marker), CD146, and CD166 (as positive MSC marker) (BD Biosciences), or isotype-matched control immunoglobulin Gs (IgGs; Southern Biotechnology Associates) and subjected to flow cytometric analysis[9] using a Beckman Coulter flow cytometer and FACScan program (BD Biosciences).

Biomaterial fabrication and cell encapsulation

Custom-made RGD-coupled alginate with high glucuronic acid content (G/M: 70/30) (GRGDSP-coupled high G alginate; Novatech; NovaMatrix FMC Biopolymer) was utilized in this study. Alginate was dissolved in deionized water to a concentration of 1% (w/v) and then purified with activated charcoal (0.5 g charcoal/g alginate) to remove organic impurities. Following charcoal treatment, the alginate solution was passed through 0.22-μm filters, lyophilized within Steriflip conical tubes (Millipore), and aliquoted, all under sterile conditions. Next, the alginate was partially oxidized to increase its degradability by producing hydrolytically labile bonds in the polysaccharide. Briefly, in a 500 mL flask, purified sodium alginate (2.0 g) was dissolved in double-distilled water (40 mL) while being stirred. Subsequently, 0.5 M solution of sodium periodate (Sigma-Aldrich) was added and the flask was stirred at ambient temperature in a dark room for 24 h. Ethylene glycol (Sigma-Aldrich) was then added to the reaction mixture to reduce any unreacted periodate. The flask was again stirred for 2 h at ambient temperature and the solution was filtered. While being held under reduced pressure, the solution was then concentrated and freeze-dried.

PDLSCs and GMSCs, as well as hBMMSCs serving as a positive control, were encapsulated in alginate at a density of 2×10^6 cells/mL of alginate solution. Microbeads were formed using a microfluidic device with a two-channel fluid jacket microencapsulator for bubble formation equipped with a micropipette. Using syringe pumps, alginate (200 μL/h; Sigma) was injected into channel 2 of the device and soybean oil (10 mL/h; Sigma) was injected into channel 1 (Fig. 2a). Glass syringes (Hamilton) were filled with the fluids and connected to the device using PEEK tubing (I.D. = 0.762 mm). Alginate droplets were sheared off by the soybean oil, allowed to flow out of the device through channel 3, and dropped into a petri dish containing 100 mM calcium chloride solution to form microbeads. The extrusion rates of the pumps were optimized to obtain spheres of uniform shape and size. The alginate droplets cross-linked and formed beads, and the resulting constructs were incubated at 37°C for 45 min to form completely cross-linked spheres. The spheres were then washed three times in nonsupplemented Dulbecco's Modified Eagle Medium. No stem cells were visible in the wells, confirming the encapsulation of the stem cells within the hydrogel spheres. Alginate microcapsules produced without stem cells were used as the negative control in this study.

Confocal laser scanning microscopy

The cell–matrix interactions of encapsulated MSCs in alginate microspheres were further characterized using confocal laser scanning microscopy (CLSM) (Fluoview FV10i; Olympus Corp.). Encapsulated MSCs after 1 week of culturing in regular media were fixed in 4% paraformaldehyde, washed in PBS, and permeabilized by incubation in 0.1% Triton X-100. MSCs were stained for cytoskeleton F-actin with Alexa Fluor 568 phalloidin (Invitrogen) and counterstained with 4′,6-diamidino-2-phenylindole.

Cell viability

Viability of the encapsulated stem cells was determined using a live/dead assay kit (Invitrogen) after the alginate microcapsules were cultured for 1, 3, 7, and 14 days according to the manufacturer's instructions. A fluorescence microscope (Olympus IX71; Olympus) was used to observe the cells. Five microspheres per group were examined and the numbers of green (live) and red (dead) cells were counted in each bead. The percentage of live cells and live cell density were determined from five independent specimens for each experimental group using NIH Image-J software (NIH).

Additionally, in order to measure stem cell viability in the alginate beads, a 3-(4,5-dimethylthiazol-2-yl)-2, 5-diphenyltetrazolium bromide (MTT) assay was utilized. Briefly, after 1, 3, 7, and 14 weeks of culturing in regular media, the MTT solution was added to the media and the encapsulated cells were incubated for 5 h at 37°C with 5% CO_2. The media were then removed, the hydrogel microspheres were homogenized, and Formosan crystals formed during this process were extracted by adding 0.5 mL of dimethyl sulfoxide. After the mixture was incubated for 40 min, the solution was transferred into 96-well plates, and the absorbance was measured at 570 nm using a microplate reader. The MTT absorbance was obtained at different time intervals, and normalized to the absorbance of alginate containing the same type of stem cells measured at day 1. Six independent specimens for each experimental group were tested at each time interval.

In vitro *osteogenic differentiation assay*

Encapsulated MSCs were cultured in osteogenic media containing 2 mM β-glycerophosphate (Sigma-Aldrich), 100 μM L-ascorbic acid 2-phosphate, and 10 nM dexamethasone (Sigma-Aldrich). After 4 weeks of osteogenic induction, the cultures were stained with xylenol orange. In addition, the expression of Runx2 and ALP was assayed by western blot analysis. Alginate microspheres without cells were used as a negative control.

Evaluation of in vitro *mineralization using fluorescent dye*

Xylenol orange, a fluorescent probe that chelates to calcium and stains mineral red, was used for osteogenic characterization. Briefly, 2 mL of 1 mM xylenol orange was added and samples were incubated overnight. Fluorescence images were collected for each sample and mineralized area was calculated using ImageJ software.

Western blot analysis

After 4 weeks of culturing in the osteogenic induction media, stem cell–alginate constructs were dissolved in citrate buffer (6% w/v, pH 7.4). Protein was extracted using M-PER

mammalian protein extraction reagent (Thermo). Nuclear protein was obtained using NE-PER nuclear and cytoplasmic extraction reagent (Thermo Scientific). The extracted protein was applied to and separated on 4–12% NuPAGE gel (Invitrogen) and then transferred to Immobilon™-P membranes (Millipore). The membranes were blocked with 5% nonfat dry milk and 0.1% tween-20 for 1 h, followed by incubation with primary antibodies (Runx2 and ALP with 1:200 dilution; Santa Cruz Biosciences) at 4°C overnight. Horseradish peroxidase (HRP)-conjugated IgG (Santa Cruz Biosciences; 1:10,000) enhanced with a SuperSignal® West Pico Chemiluminescent Substrate (Thermo Scientific) was used to treat the membranes for 1 h. The bands were detected on BIOMAX MR films (Kodak). The membranes were stripped and reprobed with an antibody directed against the housekeeping gene beta-actin (Abcam) to ensure that equal mass was loaded to each lane. The chemiluminescent reagent (Amersham Life Science) was added to the membrane for 1 min and exposed to X-ray film for variable periods (Thermo Scientific) to produce images.

In vivo *transplantation*

Approximately 4×10^6 *ex vivo*–expanded PDLSCs, GMSCs, or hBMMSCs were encapsulated in alginate hydrogel microspheres according to methods described previously and then transplanted into a 5-mm-diameter defect in the calvaria of 5-month-old Beige nude XID III (*NU/NU*) mice (Harlan Laboratories). These immunocompromised mice were selected in order to avoid potential immunogenic and graft-rejection responses as all the stem cells in this study were of human origin. These procedures were performed in accordance with the specifications of an approved small animal protocol (10941) at the University of Southern California. A total of 16 immunocompromised mice were used across four groups, including the PDLSC experimental group ($n = 4$), GMSC experimental group ($n = 4$), hBMMSC positive control group ($n = 4$), and cell-free alginate negative control group ($n = 4$). The required number of animals in these experiments was determined according to power analysis for statistical significance. Animals were sacrificed after 8 weeks.

Microcomputed tomography analysis

Right before harvesting the tissue, the reconstructed calvarial defects were examined with a high-resolution microcomputed tomography (CT) system (MicroCAT II; Siemens Medical Solutions Molecular Imaging) in order to evaluate the healing and morphology of the defects. The specimens were scanned at widths of every 10 μm at 60 kV and 110 μA at a spatial resolution of 18.676 μm (voxel dimension) and three-dimensional histomorphometric analysis was performed. The bone volume fraction (bone volume/total volume) of newly regenerated bone for each specimen was calculated using Amira software (Visage Imaging, Inc.).

Histology and immunohistochemistry

For histological examination, cranial specimens were fixed in 10% formalin solution and then decalcified with 10% ethylenediaminetetraaceticacid for 4 weeks. Samples were then dehydrated in an ascending series of ethanol and embedded in paraffin. Six-micrometer sections were cut using a microtome and mounted on glass slides. Four randomly selected cross-sections from each implant were stained with hematoxylin and eosin (H&E) or Masson's trichrome.

For immunohistochemical analysis, de-paraffinized sections were washed, and endogenous peroxidase activities were quenched by immersing in 3% H_2O_2/methanol for 15 min. Sections were then incubated with primary antibodies (1:200–1:300 dilution) for 1 h. Rabbit antibodies used for immunohistochemistry were anti-osteocalcin (OCN; Millipore; 1:200 dilution) and anti-Runx2 (Santa Cruz Biotechnology; 1:100 dilution). Other sections, still embedded in paraffin, were incubated with specific primary antibodies for human mitochondria (mouse antibody anti-human mitochondria; Chemicon) with 1:200 dilution and detected using the universal immunoperoxidase (HRP) ABC kit (Vector Laboratories). Subsequently, sections were counterstained with hematoxylin.

Statistical analysis of data

Quantitative data are expressed as mean ± standard deviation. The Kruskal–Wallis rank sum test was utilized to analyze the obtained data at a significance level of $\alpha = 0.05$.

Results

In vitro *characterization of dental-derived MSCs*

To address our hypothesis that stem cells extracted from human PDL and gingiva can contribute to bone formation *in vitro* and *in vivo*, we first extracted human PDLSCs and GMSCs from healthy patients between the ages of 18 and 25 years. A CFU-F assay was performed to assess the colony-forming ability of the newly isolated stem cells. PDLSCs and GMSCs showed significantly higher numbers of single-colony clusters (CFU-F) than that of hBMMSCs (Fig. 1a). The stem cells were expanded *in vitro* until passages 2–6 for further experiments. To identify whether the isolated cells were MSC-like, we performed flow cytometric analysis. The cytometric analysis demonstrated that the human PDLSCs and GMSCs expressed specific MSC markers CD146 and CD166, but not the hematopoietic lineage marker CD34 (Fig. 1b). The statistical analysis of data showed that these two types of dental MSCs exhibited similar expression profiles of MSC markers similar to those of hBMMSCs (Fig. 1c). These results confirmed the stem cell properties of both types of dental-derived MSCs through passages 2–6 (Fig. 1c).

Next, we examined the morphology and *in vitro* growth properties of the three cell types (Fig. 1d). Similar to hBMMSCs, human PDLSCs and GMSCs adhered to culture dishes and organized as single CFUs. PDLSCs and GMSCs isolated from human subjects showed MSC-like fibroblast CFUs. Similar to other types of dental MSCs (e.g., dental pulp stem cells), PDLSCs and GMSCs showed significantly higher proliferation rates than hBMMSCs. PDLSCs and GMSCs were more than 90% confluent after 72 h of culturing while hBMMSCs were < 50% confluent (Fig. 1e).

Alginate microencapsulation maintains stem cell viability

The alginate microspheres fabricated for the current study had an average diameter of 427 μm, ranging from 196 to 581 μm (Fig. 2a, b). In general, the microspheres exhibited

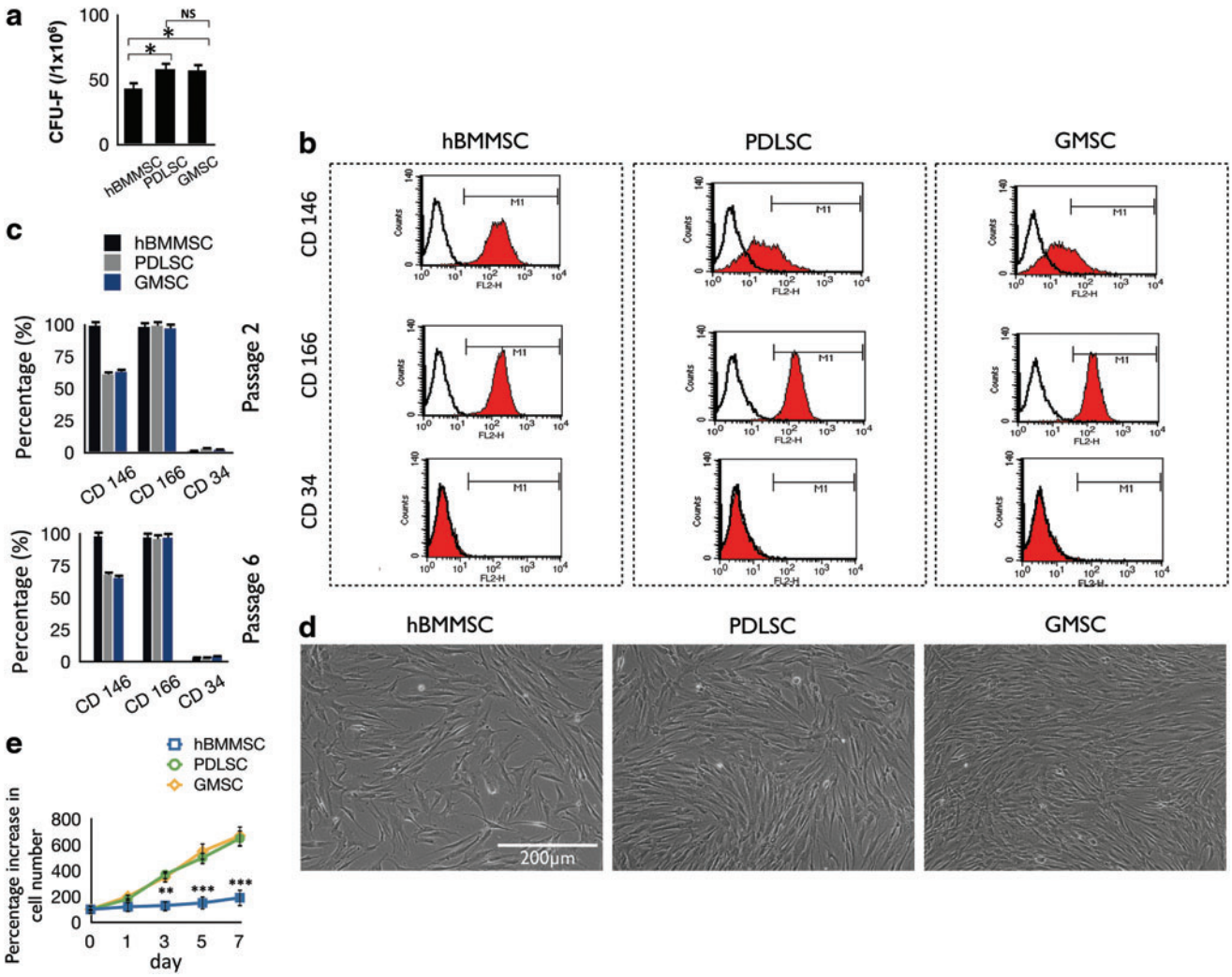

FIG. 1. **(a)** Generation of colony-forming units in cultures seeded with 1×10^6 bone marrow mesenchymal stem cells (BMMSCs), periodontal ligament stem cells (PDLSCs), and gingival mesenchymal stem cells (GMSCs) at a low density for 10 days. **(b)** Expression of cell surface markers on stem cells (passage 2) as determined by flow cytometric analysis. **(c)** Quantification of percentage of cells that express stem cell markers determined by flow cytometry (mean ± standard deviation). The results are representative of at least five independent experiments from passages 2–6. **(d)** Comparison of the morphology and growth properties of PDLSCs, GMSCs, and human BMMSCs (hBMMSCs). **(e)** Proliferation and cell counts of PDLSCs, GMSCs, and hBMMSCs ($n=5$). NS, not significant. *$p<0.05$, **$p<0.01$, ***$p<0.001$. Color images available online at www.liebertpub.com/tea

spherical shape and a narrow diameter distribution. In addition, the stem cells were round in shape and evenly dispersed inside the alginate microbeads. After 1 week of culturing, cell clustering became evident, while the alginate microspheres retained their spherical shapes. Additionally, morphology and matrix interaction of encapsulated MSCs were analyzed using CLSM by staining F-actin. Round MSCs with short cytoplasm extensions around them were observed, confirming interaction between the MSCs and the alginate hydrogel matrix (Fig. 2c).

The viability of the stem cells was not adversely affected by the application of the microfluidic device and the carrier oil, as demonstrated by the live/dead staining (Fig. 2d). Live cells in this assay are stained green with calcein-acetoxymethyl, indicating intracellular esterase activity, and the dead cells are stained red with ethidium homodimer-1, indicating loss of plasma membrane integrity. Quantitatively, no statistical differences were observed ($p>0.05$) between the percentages of live cells across the experimental and positive control groups. All showed high degrees of viability of MSCs in alginate microspheres after 4 weeks of *in vitro* culturing. More than 95% of encapsulated cells were alive at the initial point of encapsulation and 75% of cells were still alive after 2 weeks of culturing (Fig. 2e). Moreover, as tissue formation occurred during the later stages of culturing in the differentiation induction media, cell viability still remained high and necrotic cores were not observed within the aggregates, demonstrating that nutrient mass transport limitations were not experienced within the hydrogel microspheres of this size. However, the viability of MSCs in larger (1-mm average diameter) alginate microspheres without RGD was significantly lower ($p<0.05$; Fig. 2e).

Further, in order to quantitatively measure *in vitro* alginate microencapsulation system cytotoxicity and stem cell

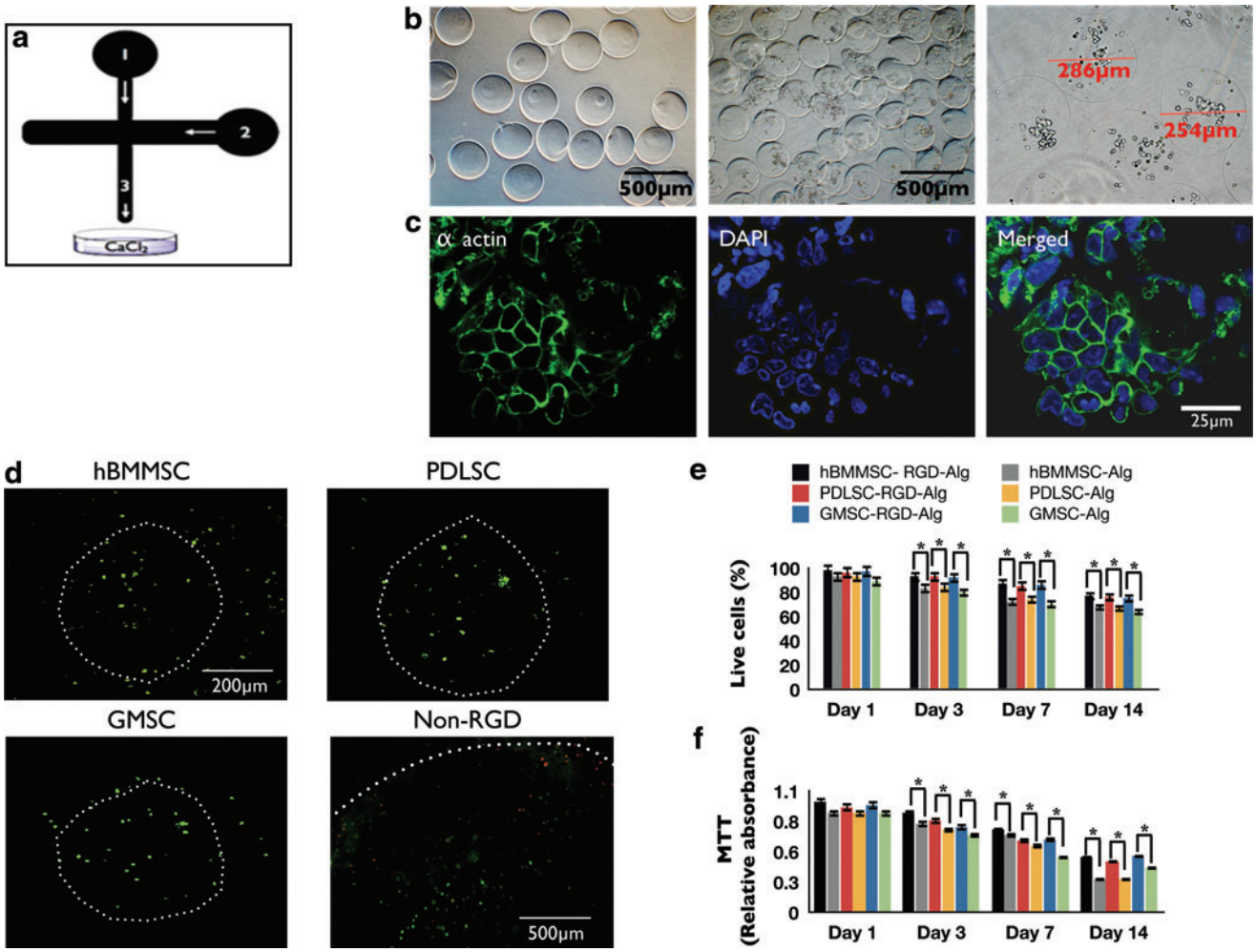

FIG. 2. **(a)** Schematic representation of microfluidic device. Channel 1: alginate injection channel; Channel 2: soybean oil injection channel. Alginate droplets were sheared off by the soybean oil and flowed out of the device through Channel 3. **(b)** Microspheres produced by the microfluidic device. The diameter of the microspheres was between 196 and 581 μm (scale bar = 500 μm). **(c)** Cytoskeleton organization of MSCs encapsulated in alginate microspheres stained with phalloidin Alexa Fluor 568 for F-actin (green) and 4′,6-diamidino-2-phenylindole (DAPI, blue) for nucleus. **(d)** Live/dead staining of the stem cell microspheres after 1 week of culturing (scale bar = 200 μm). White dots show the peripheries of each microcapsule. Note the larger diameter of the non-RGD-containing alginate microsphere (with PDLSCs) with average diameter of 1 mm, fabricated via traditional methods.[18,19] Larger microspheres show more dead positive cells after 1 week than RGD-coupled microspheres fabricated using microfluidics. **(e)** Viability of the encapsulated PDLSCs, GMSCs, and hBMMSCs: live/dead staining, percentage of live cells in either RGD-coupled alginate microspheres or in alginate microspheres without RGD. **(f)** 3-(4,5-Dimethylthiazol-2-yl)-2, 5-diphenyltetrazolium bromide (MTT) assay of metabolic activity of cells. No significant difference was observed between the stem cell groups at each time interval. *$p < 0.05$. Color images available online at www.liebertpub.com/tea

viability, dental MSC constructs were treated with MTT. All the stem cell alginate constructs showed high MTT absorbance, indicating high metabolic activity and cell viability after up to 2 weeks of culturing (Fig. 2f). These results show that conditions for PDLSCs, GMSCs, and hBMMSCs were favorable in the smaller-diameter, biodegradable alginate microspheres with an average diameter of 427 μm. MSCs encapsulated in larger-diameter alginate hydrogel spheres without RGD showed significantly reduced cell metabolic activity (Fig. 2f).

Osteogenic differentiation of dental MSCs in vitro

In order for PDLSCs and GMSCs to be useful for *in vivo* bone regeneration, it is necessary to verify that they have the potential to differentiate into osteogenic tissue. Dental MSCs after passage 4 were encapsulated in alginate microspheres and the culture media were changed to osteogenic differentiation media consisting of L-ascorbate-2-phosphate, glucocorticoid, dexamethasone, and inorganic phosphate. After 4 weeks of culturing in the osteogenic media, PDLSCs, GMSCs, and hBMMSCs exhibited positive xylenol orange labeling (Fig. 3a, b). As expected, hBMMSCs formed more mineralized area than PDLSCs ($p < 0.05$) or GMSCs ($p < 0.01$) (Fig. 3c). Among the stem cells derived from oral tissues, PDLSCs showed a significantly higher fraction of mineralized tissue area than GMSCs ($p < 0.05$). These results showed the moderate osteogenic capacity of these PDLSCs in comparison to the high osteogenic differentiation capacity of hBMMSCs. However, GMSCs exhibited significantly lower

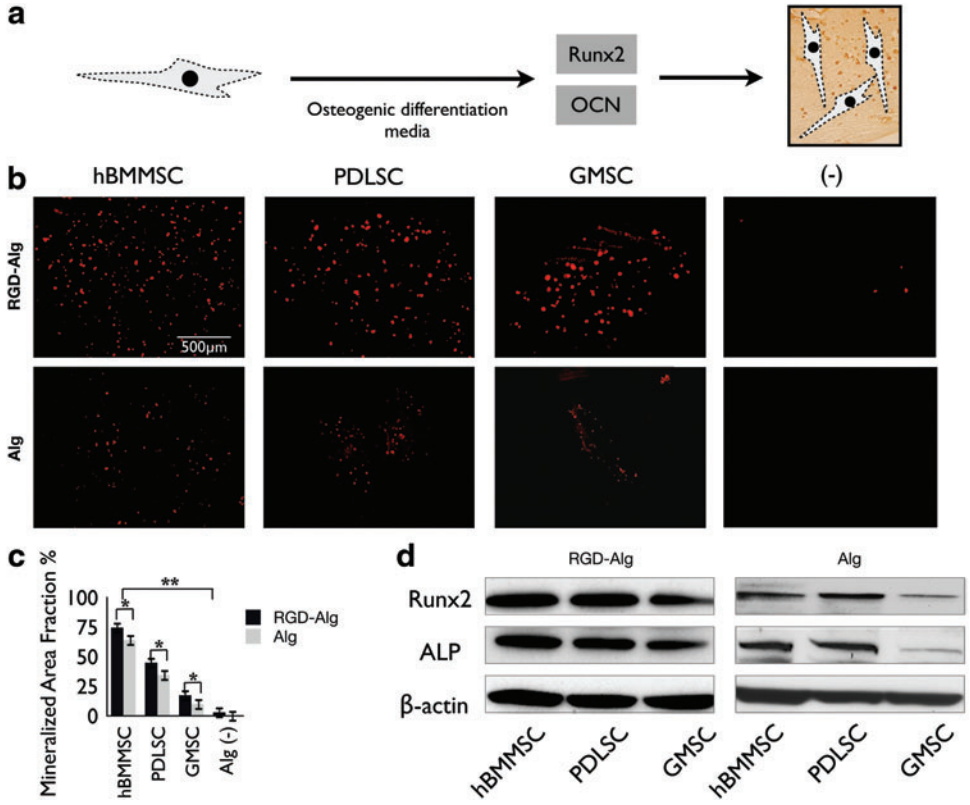

FIG. 3. **(a)** Simple schematic representation of the transcription factors regulating the differentiation of MSCs and osteogenesis. **(b)** Osteodifferentiation and mineralization of encapsulated PDLSCs, GMSCs, and hBMMSCs in alginate *in vitro* after 4 weeks of culturing in osteogenic differentiation media. The specimens were stained by xylenol orange and emitted red fluorescence. **(c)** Mineralization area fraction was defined as the area of stained mineralization divided by the total area of the field of view of the image. **(d)** Western blot analysis of the expression of ALP and Runx2. $*p<0.05$, $**p<0.01$. Color images available online at www.liebertpub.com/tea

($p<0.05$) bone regenerative potential in comparison to hBMMSCs or even PDLSCs. The positive effects of the presence of RGD groups and a smaller diameter of alginate microspheres on the degree of osteogenesis of MSCs *in vitro* were also confirmed. Further, the results of our fluorescent staining correlated well with our western blot analysis results. An increase in the expression level of osteoblast-specific molecules, including Runx2 and ALP, was detected by western blot analysis after 4 weeks of culturing in osteogenic differentiation media, compared with expression levels of MSCs in alginate microspheres without RGD and an average diameter of 1 mm (Fig. 3d). The alginate microcapsules without cells were used as the negative control in this study. Taken together, these data prompted us to test the bone regeneration capacity of PDLSCs and GMSCs encapsulated in RGD-coupled alginate microspheres in an *in vivo* calvarial defect model.

Encapsulated dental MSCs contributed to bone regeneration in calvarial defect model

To test the bone regeneration ability of PDLSCs or GMSCs encapsulated in RGD-modified alginate microspheres *in vivo*, we used a 5-mm critical-sized calvarial defect in immunocompromised mice. This animal model was chosen due to its close relationship to craniofacial regeneration and the neural crest origin of the calvarial cells. To avoid self-repair by the host, a nonhealing, full-thickness defect of 5 mm in diameter was made.[42,43] To assess whether PDLSCs and GMSCs were able to contribute to bone tissue regeneration *in vivo*, we transplanted 4×10^6 human PDLSCs or GMSCs encapsulated in RGD-coupled alginate microspheres into the defect sites (Fig. 4a). Encapsulated hBMMSCs were used as the positive control, while alginate hydrogel alone was used as the negative control in this animal model. To evaluate new bone formation and the development of bone within the defects, micro-CT and histological analyses were utilized. The quantity and quality of bone regenerated in the calvarial defect sites were evaluated and compared after 8 weeks. Micro-CT analysis (Fig. 4b) demonstrated significant amounts of bone fill and repair in defects transplanted with PDLSCs in comparison to the negative control group ($p<0.05$). Quantitative analysis of micro-CT data revealed that GMSCs exhibited significantly lower ($p<0.05$) bone regenerative potential in comparison to hBMMSCs or even PDLSCs. As expected, the positive control group (hBMMSCs) formed the largest amount of bone ($p<0.05$; Fig. 4c). The negative control group with transplants containing alginate hydrogel alone did not regenerate a significant degree of calvarial bone during the experimental period; the amount of new bone was significantly less than what was observed in sites transplanted with PDLSCs, GMSCs, or hBMMSCs ($p<0.01$).

Histological evidence further supported the micro-CT observations. Results of histologic staining with H&E (not shown) and trichrome demonstrated significant bone fill within calvarial defects transplanted with encapsulated PDLSCs, while the GMSCs encapsulated in RGD-coupled alginate microspheres showed significantly lower amounts of bone fill (Fig. 4d). These results correlated well with the micro-CT data. However, oral MSC-mediated bone lacked hematopoietic marrow elements, which were found routinely in bone generated in hBMMSCs, as has been reported previously.[5,30] Trichrome staining revealed viable mature woven bone formation with a lamellate pattern, and osteocytes within lacunae were evident for PDLSCs and GMSCs

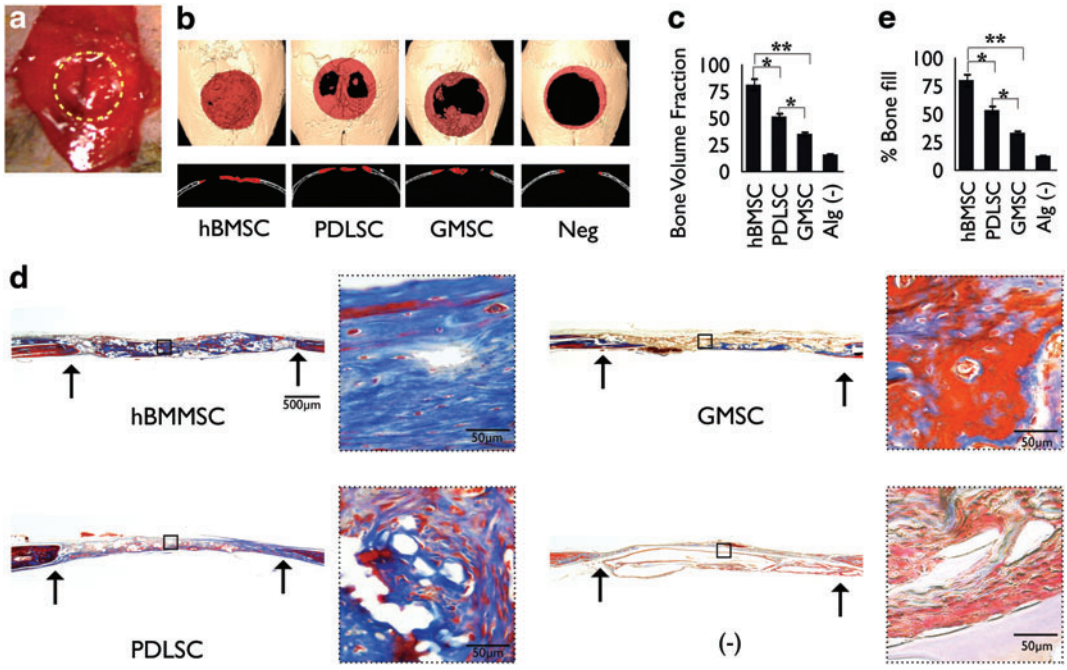

FIG. 4. *In vivo* calvarial defect model in mice. **(a)** Calvarial defects (5 mm) were generated along the yellow dots in nude mice and encapsulated PDLSCs, GMSCs, or hBMMSCs were transplanted in the defect sites. **(b)** Microcomputed tomography (CT) three-dimensional reconstruction of bone repair in mouse calvarial defects implanted with PDLSCs, GMSCs, or hBMMSCs encapsulated in RGD-modified alginate. Red dots represent the periphery of the defect site. **(c)** Semiquantitative analysis of bone formation via micro-CT images. **(d)** Histomicrographs (trichrome staining) of mouse calvarial bone defects after 8 weeks of transplantation. Arrows indicate the boundaries of defects. **(e)** Histomorphometric analysis of calvarial defects showing the relative amount of bone formation. $^{*}p<0.05$, $^{**}p<0.01$, $n=4$ for each group. Color images available online at www.liebertpub.com/tea

as well as hBMMSCs. No evidence of dystrophic calcifications was found in our experimental sections. On the other hand, further histological analysis revealed that sites implanted with the negative control alginate hydrogel contained fibrovascular connective tissue consisting of interwoven bundles of collagenous fibers and unresorbed alginate hydrogel (Fig. 4d).

Next, the percentage of osteoid bone coverage was measured within histomicrographs. Our histomorphometric analysis indicated that hBMMSCs consistently formed significantly higher ($p<0.05$) amounts of mineralized tissue to repair the defects compared with PDLSCs and GMSCs (Fig. 4e). Quantitative analysis demonstrated that the amount of bone repair by PDLSCs was significantly greater than the amount of repair by GMSCs ($p<0.05$). In addition, as expected, the positive control group (hBMMSCs) formed the largest amount of bone ($p<0.05$), while GMSCs exhibited significantly lower values in comparison to hBMMSCs ($p<0.01$). These findings imply a potential functional role for human PDLSCs and GMSCs in bone tissue regeneration.

To further characterize dental-MSC-mediated bone formation, we utilized immunohistochemical staining. Our immunohistochemical staining clearly revealed that human PDLSCs and GMSCs, as well as hBMMSCs, actively contribute to bone formation. This is confirmed by the presence of human-specific osteogenic markers, including Runx2 and OCN (Fig. 5a). Strong expression of Runx2 and OCN was found in areas of new bone formation within defect regions treated with PDLSCs, as well as the hBMMSC positive control group, while GMSCs showed milder expression of these osteogenic markers (Fig. 5a). Further, the human origin of cellular components of the transplants was confirmed with specific anti-human mitochondrial antibody staining (Fig. 5a). In addition, semiquantitative analysis showed that a considerably higher percentage of cells were positive under anti-Runx2 and -OCN antibody staining in the dental MSC experimental groups than in the control group (Fig. 5b). No evidence of cells positive for anti-Runx2 and -OCN antibodies was observed for the negative control group.

Discussion

In this study, we developed an injectable RGD-coupled alginate-hydrogel microsphere as a stem cell delivery system for potential application in bone tissue engineering. We demonstrated that this system supported the viability, metabolic activity, and differentiation of encapsulated PDLSCs and GMSCs. *In vivo* mineralization and bone repair were observed in a calvarial defect mouse model using micro-CT and histological analyses.

There are many disadvantages associated with the current treatment modalities for bone regeneration in craniofacial reconstructive surgeries and regenerative medicine, as previously mentioned.[41,44,45] We demonstrate here that MSCs derived from orofacial tissues show promise as a therapeutic option and do not suffer from the drawbacks of the current bone regeneration techniques.[42,43,46] From a practical perspective, gingival tissues (and to some extent the periodontal ligaments) provide superior sources of MSCs considering their accessibility and ready availability for autologous transplantation. These tissue sources provide a unique reservoir of stem cells from accessible tissue resources.[7,42] Using

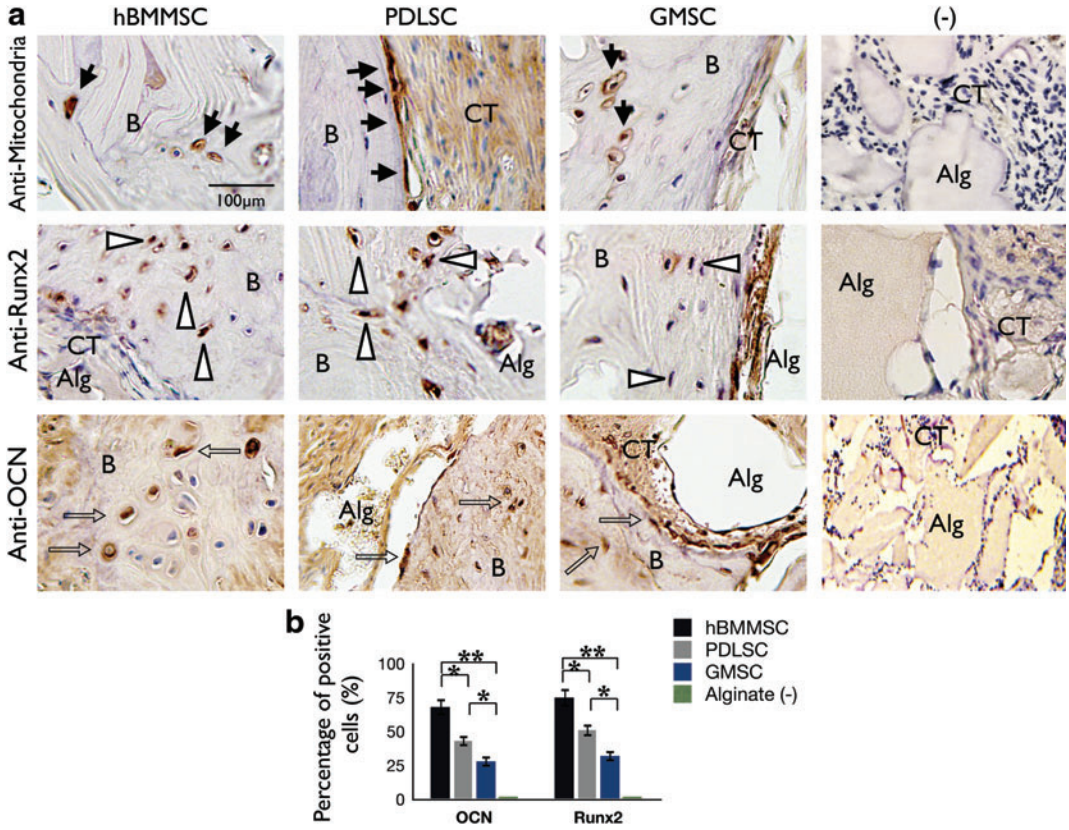

FIG. 5. Characterization of the origin and fate of PDLSCs and GMSCs after transplantation. **(a)** Upper panel: The cells of human origin were confirmed by immunohistochemical staining with a specific antibody for human mitochondria (black arrows). After 8 weeks of transplantation in immunocompromised mice, both PDLSCs and GMSCs were able to form bone. **(b)** Osteogenic cells were positive for anti-osteocalcin (OCN; middle panel, open arrows in black) and Runx2 (lower panel, white arrows) antibody staining, while negative control (−) immunohistochemical staining results failed to express any of these osteogenic markers. **(b)** Semiquantitative analysis of percent of positive cells for anti-OCN and anti-Runx2 antibodies via immunohistochemical staining images. $*p < 0.05$, $**p < 0.01$. Scale bar = 100 μm. Color images available online at www.liebertpub.com/tea

PDL or gingival tissues collected from one patient, it is possible to extract and identify many stem cells. Therefore, human PDLSC- or GMSC-mediated tissue regeneration might be considered as a promising cellular-based modality of bone tissue engineering. However, according to the results of the current study, the earlier-mentioned benefits of PDLSCs or GMSCs are offset by the milder bone regeneration capacity, specially for GMSCs when compared with hBMMSCs.

Our previous studies demonstrated that alginate hydrogel is a promising scaffold for dental MSCs in the process of bone tissue engineering.[19,20] However, spheres that were created in our previous studies had an average diameter of 1 mm, which is far beyond the diffusion limit of oxygen. To address this issue, in this study, microfluidic technology was utilized to achieve an average diameter of < 500 μm. This strategy enhanced the transport of nutrients, oxygen, and waste products through the matrix of microspheres, maintaining high cell viability. In the current study, in addition to reducing the diameter of the alginate microspheres to < 500 μm, RGD-coupled alginate hydrogel was also utilized to provide a suitable chemical microenvironment for dental MSCs by presenting ligands that specifically bind to cell receptors.[44,45,47,48,49] Cell viability analysis and MTT assays showed that up to 80% of encapsulated cells were viable while immobilized in these new alginate microspheres, which suggests a favorable inward flux of nutrients and sufficient levels of oxygen to the cell cluster within the alginate. Thus, we observed very high cell viability and metabolic activity after up to 2 weeks of culturing. The RGD-modified alginate microspheres were able to support the PDLSCs and GMSCs with high cellular compatibility. Further, it has been reported that presentation of RGD tripeptide to alginate scaffold can promote osteoblast proliferation, leading to increased bone regeneration capacity.[24,28] In our current *in vitro* study, we confirmed that RGD-modified alginate microspheres containing dental MSCs indeed produced significantly more mineralized tissue than was generated by unmodified alginate hydrogel.

We demonstrated the possibility of osteo-differentiation of PDLSCs and GMSCs encapsulated in RGD-modified alginate microspheres both *in vitro* and *in vivo*. PDLSCs or GMSCs encapsulated in RGD-coupled alginate after 4 weeks of osteogenic induction *in vitro* showed significantly higher degrees of osteo-differentiation than MSCs encapsulated in non-RGD-coupled alginate, as confirmed by XO staining and western blot analysis (Fig. 3a–d). Further, when either PDLSCs or GMSCs were transplanted into a critical-size calvarial defect in mice, they generated bony tissue to repair the defect. These newly formed bony tissues were

immunopositive for Runx2 and OCN antibodies. The human origin of cellular components of the transplants was confirmed through immunostaining with specific antibodies against human mitochondria (Figs. 4 and 5).

In recent studies, it has been shown that culturing PDLSCs in osteogenic media for 14 days prior to implantation might facilitate the accumulation of osteogenic growth factors within the scaffold and improve cell adaptation to the substrate, leading to improved *in vivo* bone repair.[17,18] However, in the current study, stem cells were not cultured in osteogenic media prior to surgical transplantation; yet, encapsulated PDLSCs and GMSCs promoted bone regeneration *in situ* without any premineralization. Additionally, we confirmed that the presence of RGD tripeptide and the small diameter of alginate microspheres are crucial factors for MSC survival and fate determination.

It has to be mentioned that if autologous dental MSCs are to be used, then they have to be harvested during a minor surgical procedure. If dental MSCs are instead to be obtained from discarded tissue samples, then stem cell banking should be considered; a topic that is beyond the scope of this article. Altogether, our findings demonstrated that PDLSCs and GMSCs in RGD-coupled alginate possess osteogenic differentiation potential both *in vitro* and *in vivo* that could be used to mediate bone regeneration. We demonstrate that our alginate delivery system, when utilized to encapsulate dental MSCs, is capable of repairing critical-size calvarial defects in immunocompromised mice.

Conclusions

In this study we reported the development of an injectable RGD-coupled alginate microsphere delivery system for PDLSCs and GMSCs. PDLSCs encapsulated in RGD-coupled alginate microspheres showed moderate capacity for osteodifferentiation both *in vitro* and *in vivo*, while GMSCs showed significantly lower osteogenic differentiation capability when compared with hBMMSCs or even PDLSCs. To our knowledge, this is the first time that RGD-coupled alginate hydrogel has been used to deliver PDLSCs and GMSCs in a calvarial defect animal model. The alginate was manipulated and oxidized to promote degradation into soluble oligomers, eliminating the need for an additional clinical visit to remove the scaffold. This system therefore has the potential to enhance hard tissue regeneration in order to accomplish minimally invasive dental and orthopedic surgeries. This technology is a promising candidate for accelerated craniofacial bone regeneration.

Acknowledgments

This work was partially supported by grants from the National Institute of Dental and Craniofacial Research (R01DE017449 and R01 DE019932 to S.S.) and a fellowship research award from the American College of Prosthodontics Education Foundation (to A.M.). The first author (A.M.) was part of NIDCR postdoctoral training grant (T90DE021982-02) and Provost's Postdoctoral Scholar Research Grant by the USC Office of Postdoctoral Affairs.

Disclosure Statement

The authors declare no potential conflicts of interest with respect to the authorship and/or publication of this article.

References

1. Sachlos, E., and Czernuszka, J.T. Making tissue engineering scaffolds work. Review on the application of solid freeform fabrication technology to the production of tissue engineering scaffold. Eur Cell Mater **5,** 29, 2003.
2. Chen, F.M., Zhang, J., Zhang, M., An, Y., Chen, F., and Wu, Z.F. A review on endogenous regenerative technology in periodontal regenerative medicine. Biomaterials **31,** 7892, 2010.
3. Monaco, E., Bionaz, M., Hollister, S.J., and Wheeler, M.B. Strategies for regeneration of the bone using porcine adult adipose-derived mesenchymal stem cells. Theriogenology **75,** 1381, 2011.
4. Gronthos, S., Mankani, M., Brahim, J., Robey, P.G., and Shi, S. Postnatal human dental pulp stem cells (DPSCs) *in vitro* and *in vivo*. Proc Natl Acad Sci U S A **97,** 13625, 2000.
5. Seo, B.M., Miura, M., Gronthos, S., Bartold, P.M., Batouli, S., Brahim, J., *et al.* Investigation of multipotent postnatal stem cells from human periodontal ligament. Lancet **364,** 149, 2004.
6. Gronthos, S., Brahim, J., Li, W., Fisher, L.W., Cherman, N., Boyde, A., *et al.* Stem cell properties of human dental pulp stem cells. J Dent Res **81,** 531, 2002.
7. Zhang, Q., Shi, S., Liu, Y., Uyanne, J., Shi, Y., Shi, S., and Le, A.D. Mesenchymal stem cells derived from human gingiva are capable of immunomodulatory functions and ameliorate inflammation-related tissue destruction in experimental colitis. J Immunol **183,** 7787, 2009.
8. Sonoyama, W., Liu, Y., Fang, D., Yamaza, T., Seo, B.-M., Zhang, C., *et al.* Mesenchymal stem cell-mediated functional tooth regeneration in swine. PLoS One **1,** 1, 2006.
9. Lindroos, B., Maenpaa, K., Ylikomi, T., Oja, H., Suuronen, R., and Miettinen, S. Characterization of human dental stem cells and buccal mucosa fibroblasts. Biochem Biophys Res Commun **368,** 329, 2008.
10. Iwata, T., Yamato, M., Zhang, Z., Mukobata, S., Washio, K., Ando, T., *et al.* Validation of human periodontal ligament-derived cells as a reliable source for cytotherapeutic use. J Clin Periodontol **37,** 1088, 2010.
11. Mitrano, T.I., Grob, M.S., Carrion, F., Nova-Lamperti, E., Luz, P.A., Fierro, F.S., *et al.* Culture and characterization of mesenchymal stem cells from human gingival tissue. J Periodontol **81,** 917, 2010.
12. Tomar, G.B., Srivastava, R.K., Gupta, N., Barhanpurkar, A.P., Pote, S.T., Jhaveri, H.M., *et al.* Human gingiva-derived mesenchymal stem cells are superior to bone marrow-derived mesenchymal stem cells for cell therapy in regenerative medicine. Biochem Biophys Res Commun **393,** 377, 2010.
13. Wang, F., Yu, M., Yan, X., Wen, Y., Zeng, Q., Yue, W., *et al.* Gingiva-derived mesenchymal stem cell-mediated therapeutic approach for bone tissue regeneration. Stem Cells Dev **20,** 2093, 2011.
14. Zhao, Y.H., Zhang, M., Liu, N.X., Lv, X., Zhang, J., Chen, F.M., and Chen, Y.J. The combined use of cell sheet fragments of periodontal ligament stem cells and platelet-rich fibrin granules for avulsed tooth reimplantation. Biomaterials **34,** 5506, 2013.
15. Man, Y., Wang, P., Guo, Y., Xiang, L., Yang, Y., Qu, Y., *et al.* Angiogenic and osteogenic potential of platelet-rich plasma and adipose-derived stem cell laden alginate microspheres. Biomaterials **33,** 8802, 2012.
16. Kaully, T., Kaufman-Francis, K., Lesman, A., and Levenberg, S. Vascularization of the conduit to viable engineered tissues. Tissue Eng Part B Rev **15,** 159, 2009.
17. Tour, G., Wendel, M., and Tcacencu, I. Cell-derived matrix enhances osteogenic properties of hydroxyapatite. Tissue Eng Part A **17,** 127, 2011.

18. Tour, G., Wendel, M., Moll, G., and Tcacencu, I. Bone repair using periodontal ligament progenitor cell-seeded constructs. J Dent Res **91,** 789, 2012.
19. Moshaverinia, A., Chen, C., Akiyama, K., Ansari, S., Xu, X., Chee, W.W., Schricker, S.R., and Shi, S. Alginate hydrogel as a promising scaffold for dental-derived stem cells: an *in vitro* study. J Mater Sci Mater Med **23,** 3041, 2012.
20. Moshaverinia, A., Chen, C., Akiyama, K., Xu, X., Chee, W.W., Schricker, S.R., and Shi, S. Encapsulated dental-derived stem cells in an injectable and biodegradable scaffold for applications in bone tissue engineering. J Biomed Mater Res Part A **101,** 3285, 2013.
21. Alsberg, A., Anderson, K.W., Albeiruti, A., Franceschi, R.T., and Mooney, D.J. Cell-interactive alginate hydrogels for bone tissue engineering. J Dent Res **80,** 2025, 2001.
22. Kretlow, J.D., Young, S., Klouda, L., Wong, M., and Mikos, A.G. Injectable biomaterials for regenerating complex craniofacial tissues. Adv Mater **21,** 3368, 2009.
23. Hill, E., Boontheekul, T., and Mooney, D.J. Designing scaffolds to enhance transplanted myoblast survival and migration. Tissue Eng Part A **12,** 1295, 2006.
24. Rowley, J.A., Madlambayan, G., and Mooney, D.J. Alginate hydrogels as synthetic extracellular matrix materials. Biomaterials **20,** 45, 1999.
25. Smidsrod, O., and Skjakbraek, G. Alginate as immobilization matrix for cells. Trends Biotechnol **8,** 71, 1990.
26. Higasi, T., Nagamori, E., Sone, T., Matsunaga, S., and Fukui, K. A novel transfection method for mammalian cells using calcium alginate microbeads. J Biosci Bioeng **97,** 191, 2004.
27. Augst, A.D., Kong, H.J., and Mooney, D.J. Alginate hydrogels as biomaterials. Macromol Biosci **6,** 623, 2006.
28. Lee, C.S.D., Moyer, H.R., Gittens, R.A., Williams, J.K., Boskey, A.L., Boyan, B.D., *et al.* Regulating *in vivo* calcification of alginate microbeads. Biomaterials **31,** 4926, 2010.
29. Evangelista, M.B., Hsiong, S.X., Fernandes, R., Sampaio, P., Kong, H., Barrias, C.C., *et al.* Upregulation of bone cell differentiation through immobilization within a synthetic extracellular matrix. Biomaterials **28,** 3644, 2007.
30. Workman, V.L., Dunnett, S.B., Kille, P., and Palme, D.D. Microfluidic chip-based synthesis of alginate microspheres for encapsulation of immortalized human cells. Biomacrofluid **105,** 1, 2007.
31. Joanicot, M., and Ajdari, A. Droplet control for microfluidics. Science **309,** 887, 2005.
32. Gautier, A., Carpentier, B., Dufresne, M., Vu, D.Q., Paullier, P., and Legallais, C. Impact of alginate type and bead diameter on mass transfer and the metabolic activities of encapsulated C3A cells in bioartificial liver applications. Eur Cell Mater **21,** 94, 2011.
33. Wang, C.C., Yang, K.C., Lin, K.H., Liu, H.C., and Lin, F.H. A highly organized three-dimensional alginate scaffold for cartilage tissue engineering prepared by microfluidic technology. Biomaterials **32,** 7118, 2011.
34. Hatch, A., Hansmann, G., and Murthy, S.K. Engineered alginate hydrogels for effective microfluidic capture and release of endothelial progenitor cells from whole blood. Langmuir **27,** 4257, 2011.
35. Anselme, K. Osteoblast adhesion on biomaterials. Biomaterials **21,** 667, 2000.
36. Gronowicz, G.A., and Derome, M.E. Synthetic peptide containing Arg-Gly-Asp inhibits bone formation and resorption in a mineralizing organ culture system of fetal rat parietal bones. J Bone Miner Res **9,** 193, 1994.
37. Xiao, G., Wang, D., Benson, M.D., Karsenty, G., and Franceschi, R.T. Role of the alpha 2-integrin in osteoblast-specific gene expression and activation of the Osf2 transcription factor. J Biol Chem **273,** 32988, 1998.
38. Ruoslahti, E., and Pierschbacher, M.D. Arg-Gly-Asp: a versatile cell recognition signal. Cell **44,** 517, 1986.
39. Boudreau, N.J., and Jones, P.L. Extracellular matrix and integrin signaling: the shape of things to come. Biochem J **339,** 481, 1999.
40. Batouli, S., Miura, M., Brahim, J., Tsutsui, T.W., Fisher, L.W., Gronthos, S., Robey, P.G., and Shi, S. Comparison of stem-cell-mediated osteogenesis and dentinogenesis. J Dent Res **82,** 976, 2003.
41. Mauney, J.R., Kirker-Head, C., Abrahamson, L., Gronowicz, G., Volloch, V., and Kaplan, D.L. Matrix-mediated retention of *in vitro* osteogenic differentiation potential and *in vivo* bone-forming capacity by human adult bone marrow-derived mesenchymal stem cells during *ex vivo* expansion. J Biomed Mater Res A **79,** 464, 2006.
42. Seo, B.M., Sonoyama, W., Yamaza, T., Coppe, C., Kikuiri, K., Lee, J.S., and Shi, S. SHED repair critical-size calvarial defects in mice. Oral Dis **14,** 428, 2008.
43. Cowan, C.M., Shi, Y., Aalami, O.O., Chou, Y., Mari, C., Thomas, R., Quarto, N., *et al.* Adipose-derived adult stromal cells heal critical-size mouse calvarial defects. Nat Biotechnol **22,** 560, 2004.
44. Bidarra, S.J., Barrias, C.C., Barbosa, M.A., Soares, R., and Granja, P.L. Immobilization of human mesenchymal stem cells within RGD-grafted alginate microspheres and assessment of their angiogenic potential. Biomacromolecules **11,** 1956, 2010.
45. Pham, Q.P., Kasper, F.K., Scott Baggett, L., Raphael, R.M., Jansen, J.A., and Mikos, A.G. The influence of an *in vitro* generated bone-like extracellular matrix on osteoblastic gene expression of marrow stromal cells. Biomaterials **29,** 2729, 2008.
46. Liu, Y., Wang, L., Kikuiri, T., Akiyama, K., Chen, C., Xu, X., Yang, R., Chen, W., Wang, S., and Shi, S. Mesenchymal stem cell-based tissue regeneration is governed by recipient T lymphocytes via IFN-γ and TNF-α. Nat Med **17,** 1594, 2011.
47. Markusen, J.F., Mason, C., Hull, D.A., Town, M.A., Tabor, A.B., Clements, M., Boshoff, C.H., and Dunnill, P. Behavior of adult human mesenchymal stem cells entrapped in alginate-GRGDY beads. Tissue Eng Part A **12,** 821, 2006.
48. Duggal, S., Frønsdal, K.B., Szöke, K., Shahdadfar, A., Melvik, J.E., and Brinchmann, J.E. Phenotype and gene expression of human mesenchymal stem cells in alginate scaffolds. Tissue Eng Part A **15,** 1763, 2009.
49. Grellier, M., Granja, P.L., Fricain, J.C., Bidarra, S.J., Renard, M., Bareille, R., Bourget, C., Amédée, J., and Barbosa, M.A. The effect of the co-immobilization of human osteoprogenitors and endothelial cells within alginate microspheres on mineralization in a bone defect. Biomaterials **30,** 3271, 2009.

Address correspondence to:
Alireza Moshaverinia, DDS, MS, PhD
Center for Craniofacial and Molecular Biology (CCMB)
Ostrow School of Dentistry
University of Southern California
2250 Alcazar Street—CSA 103
Los Angeles, CA 90033

E-mail: moshaver@usc.edu

Received: April 9, 2013
Accepted: September 10, 2013
Online Publication Date: November 5, 2013